INTERNATIONAL JOURNAL OF CLIMATOLOGY
Int. J. Climatol. **25**: 865–879 (2005)
Published online in Wiley InterScience (www.interscience.wiley.com). DOI: 10.1002/joc.1169

OBJECTIVE ANALYSES OF SEA-SURFACE TEMPERATURE AND MARINE METEOROLOGICAL VARIABLES FOR THE 20TH CENTURY USING ICOADS AND THE KOBE COLLECTION

MASAYOSHI ISHII[a,b,*], AKIKO SHOUJI[c], SATOSHI SUGIMOTO[c], and TAKANORI MATSUMOTO[c]
[a] *Global Warming Research Program, Frontier Research Center for Global Change, Yokohama, Japan*
[b] *Climate Research Department, Meteorological Research Institute, Tsukuba, Japan*
[c] *Climate Marine Department, Japan Meteorological Agency, Tokyo, Japan*

Received 8 May 2004
Revised 10 September 2004
Accepted 10 September 2004

ABSTRACT

Data for the 20th century from the International Comprehensive Ocean and Atmosphere Data Set and the Kobe Collection have been used as input data for global objective analyses of sea-surface temperatures (SSTs) and other marine meteorological variables. This study seeks a better understanding of the historical marine meteorological data and an evaluation of the quality of the data in the Kobe Collection. Objective analyses yield gridded data that are less noisy than observed data, which facilitates handling of historical data. The observed data determine the quality of the objective analyses, and quality control specified for historical data is incorporated into the objective analysis to reduce artificial errors. The objective analyses are based on optimum interpolation and reconstruction with empirical orthogonal functions. The final database produced in this study not only contains analysed values, but also analysis errors and data distributions at each time step of the objective analyses.

The analysis database contains ample information on historical observations, as well as signals of marine climate variations during the century. Time series of global mean marine temperatures and cloud cover include trends linked to global warming, and local peaks appear commonly in all the time series around the 1940s. Sea-level pressure and sea-surface wind fields show significant linear trends at high latitudes and over the North Pacific Ocean respectively. These trends seem to be artificial. An SST analysis used widely in climatological studies was verified against HadISST from the Hadley Centre and an SST analysis derived from satellite and *in situ* observations. El Niño and southern oscillation indices for the century are successfully reproduced, even though observations in the tropics are much rarer before 1950 than after 1950. Copyright © 2005 Royal Meteorological Society.

KEY WORDS: SST; marine meteorology; objective analysis; optimum interpolation; reconstruction; ICOADS; Kobe Collection

1. INTRODUCTION

Meteorologists and oceanographers have made considerable efforts to develop historical marine meteorological databases. The International Comprehensive Ocean and Atmosphere Data Set (ICOADS; Woodruff *et al.*, 1998) is a representative historical database that is now widely used in climate studies. In addition, the Kobe Collection is a Japanese contribution to historical databases (Komura and Uwai, 1992; Manabe, 1999). These historical data can be used to describe marine climates over the past 100 years. Marine meteorological data are less influenced by random noise than are land-based data because of the large thermal inertia of the oceans and ample moisture (Yamamoto and Sakai, 2000). Post-processing the observations can yield estimates of air–sea fluxes (e.g. Esbensen and Kushnir, 1981; Hellerman and Rosenstein, 1983) that are influenced by air–sea interactions in the global climate system.

* Correspondence to: Masayoshi Ishii, Global Warming Research Program, Frontier Research Center for Global Change, 3173-25 Showamachi Kanazawa-Ku, Yokohama, 236-0001, Japan; e-mail: ism@jamstec.go.jp

This study reports on daily objective analyses of sea-surface temperature (SST) and marine meteorological variables on a $1^\circ \times 1^\circ$ grid spanning the global oceans for the period from 1900 to 2001. The analyses yield data on a regular grid in time and space. Optimization reduces noise in the original data. The analyses also reveal inhomogeneities in the quality of historical observations and facilitate development of quality control procedures suitable for historical observations. Data analysed in this study include SST, sea-level pressure (SLP), vector and scalar wind, surface air temperature (AT), surface dew-point temperature (DPT), and cloud cover. AT analyses are made for both night-time AT (NAT) only and for AT during both day and night. Cloud cover analyses include separate analyses of total and low-level cloud cover.

Monthly mean analyses are derived from the daily analyses as the arithmetic average. The monthly SST analysis is verified against HadISST from the Hadley Centre (Rayner *et al*., 2003) and an SST analysis based on satellite and *in situ* observations from the National Centers for Environmental Prediction (NCEP OI.v2 SST hereafter; Reynolds *et al*., 2002). The quality of the Kobe Collection is also discussed. 'COBE' is an acronym for centennial *in situ* observation-based estimates of the variability of SSTs and marine meteorological variables, and refers to the data analysed in this study.

2. DATA AND QUALITY CONTROL

2.1. Data sources

The database of *in situ* observations used in this study includes about 160 million reports from the Kobe Collection, ICOADS release 2, a buoy dataset, and about 14 million weather reports delivered via the global telecommunication system (GTS). The buoy dataset was compiled by the Marine Environmental Data Service (MEDS) of Canada. Some MEDS data are already included in ICOADS, but the latest MEDS dataset (May 2000 edition) is larger than the MEDS dataset in ICOADS. Therefore, MEDS data in ICOADS were replaced by the latest MEDS data. ICOADS data include data through to 1997; GTS data are used for 1998 to 2000. Figure 1 shows the number of reports and available data for each year. The number of annual reports is less than one million per year before 1950. It subsequently increases dramatically. There are few DPT observations in comparison with the number of other observations for all decades. Similarly, there are relatively few SLP data before 1930. The curves in the figure are spread in recent decades, since buoy observations have become more commonplace. The spatial coverage of observations is poor before 1950, especially in the Southern Hemisphere and in the equatorial Pacific.

2.2. Sea ice

Sea-ice concentration (SIC) is used to create the SST climatology and make the SST analysis. Here, a proxy of SST in polar regions is derived from SIC using a statistical relationship between SIC and SST. The relationship is given by a quadratic function, $\mathrm{SST} = aI^2 + c$, where coefficients a and c are constants that are defined monthly and geographically. If SIC exceeds 95%, then SST is set to a minimum value, $-1.8\,^\circ\mathrm{C}$. Additional satellite-derived SSTs compiled by the National Environmental Satellite, Data, and Information Service of NOAA, are used to compute a and c. Note that satellite-derived data are only used to estimate SIC in the SST analysis. The linear term in the quadratic function is neglected so that the function ensures a maximum SST along the sea-ice margin. Moreover, it is difficult to obtain reliable values of two coefficients with few and noisy SST observations in polar regions. The linear term is, however, considered in both HadISST and NCEP OI.v2 SST.

SIC in this study is derived each day on a $1^\circ \times 1^\circ$ grid based on brightness temperatures from the Nimbus-5 scanning multichannel microwave radiometer (SMMR; October 1978 to July 1987) and the special sensor microwave imager (SSM/I; August 1987 to December 2000) using NASA-team algorithms (Cavalieri *et al*., 1984, 1991). Corrections proposed by Cavalieri *et al*. (1999) are applied to SMMR data to mediate the discontinuity in SIC observations between SMMR and SSM/I data, and to data from both satellites to remove measurement errors. Corrections are not applied for summer SIC measurement errors (such as noise) and

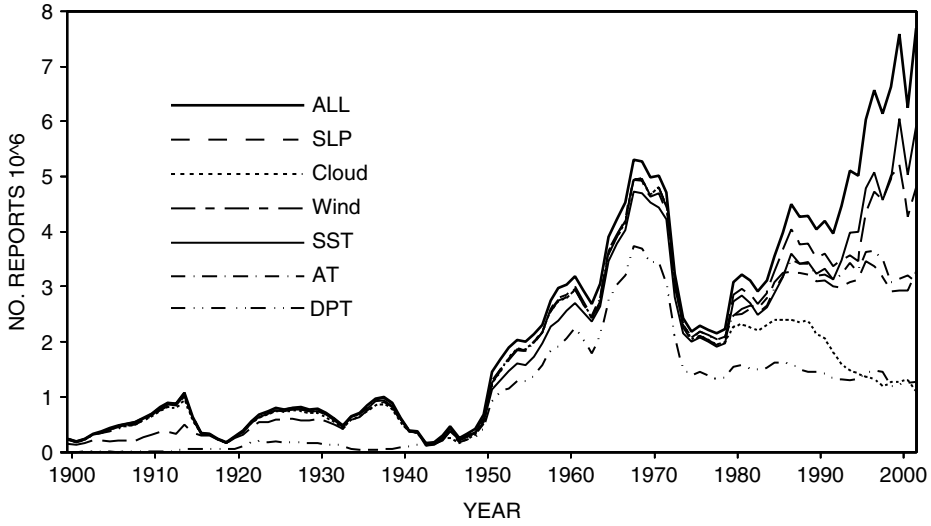

Figure 1. Time series of the annual number (unit 10^6) of all reports (thick solid), SLP (dash), total cloud cover (dotted), wind (long and short-dashes), SST (thin solid), AT (dash-dotted), and DPT (dash-two-dotted) available for the objective analyses

negative biases attributable to surface conditions (such as meltwater ponding and the submersion of the ice interface). Such errors produce noise in the SST analysis.

Daily SIC is interpolated for days between January 1901 to October 1978 from a monthly dataset assembled by Walsh and Chapman (2001). No adjustment between the Walsh study and the satellite sea-ice is attempted; this will be the focus of a future study. Daily SIC is created using climatology elsewhere: before December 1900 in the Northern Hemisphere and before October 1978 in the Southern Hemisphere.

2.3. Quality control

Quality control of historical data helps to define the quality of the analysed data because objective analyses are based on pure statistics. Observational biases or trends due to historical changes in the observational methods must be removed from the data. However, such removal is difficult because so-called metadata are limited and details on the historical backgrounds are not well known.

All observed data have been converted into International Marine Meteorological Tape format version 1 (IMMT; World Meteorological Organization, 1990). The format does not retain original values, but the data are in a format that is handled easily and is widely distributed (Manabe, 1999). Data are flagged if reported values are within normal ranges determined *a priori* in each latitude band or over each ocean basin, and if data are internally consistent, e.g. consistence between AT and DPT, following the minimum quality control standard (MQCS; World Meteorological Organization, 1990).

As in Ishii *et al*. (2003), observations are compared with climatology and nearby observations. If two or more observations are available in a grid box on a day, then they are merged into an averaged observation, or 'super observation'. This data-merging procedure reduces data redundancy, homogenizes the data distribution in space and time, and reduces the computational time demands of the objective analyses (White, 1995; Ishii *et al*., 2003). Observations are averaged separately for day and night in the data-merging procedure. This procedure will reduce day–night biases for marine meteorological elements.

SST biases in bucket observations before 1941 are removed with corrections that are a function of space and time since 1856 (Folland and Parker, 1995). Hanawa *et al*. (2000) studied coastal water temperatures at stations along the Japanese coast and showed that this SST correction is also effective for observations in the Kobe Collection. Recently, the UK Met Office compared ICOADS and MOHSST6 SSTs and found a positive bias in ICOADS SST around 1940 (Folland, 2003). The correction to remove that bias is not applied to the present analysis, but it will be done in a subsequent version of the analysis.

Folland *et al*. (1984) noted that NAT observations have a positive bias during World War II because of on-deck observations. Therefore, 0.5 °C is subtracted not only from NAT, but also from daytime AT and DPT observations.

Ramage (1987) noted that it can be difficult to identify biases in historical surface wind observations because of mixing in estimated winds from sailing-ship performance and sea surface roughness, and biases in the directly measured anemometer winds. The estimation of sea surface roughness by a number on the so-called Beaufort scale is common in the early decades. The Beaufort scale (World Meteorological Organization, 1970) has been faulted for underestimating weak winds and overestimating strong winds, and the scale was re-examined and modified by da Silva *et al*. (1994) and Lindau (1994). This study adopts the scale of Lindau (1994).

As the sizes of ships have increased in recent decades, the installation heights of anemometers have increased, and, consequently, measured winds have increased (Cardone *et al*., 1990). All wind speeds were adjusted to 10 m winds in this study, in consideration of atmospheric stability (Kutsuwada, 1998), to remove this trend. The anemometer installation height for 1973 to 1997 is documented in WMO publication 47 (WMO47; World Meteorological Organization, 1973–1999). Unfortunately, about 80% of all anemometer heights are unknown. For such unknown cases, the anemometer height is given by the mean height as a function of the year Y: $17.9 + 0.12(Y - 1973)$ and $17.9 + 0.31(Y - 1973)$, for years before and after 1973 respectively. The function for later years is derived from a linear fit to the anemometer heights listed in WMO47. A slope of 0.12 m/year is used in the function for earlier years because the trend is equivalent to that of platform heights in both the WMO47 and the Kobe Collection. A constant height of 5 m is used for all moored buoys.

Doubtful reports of position and date are modified by a ship track check that was developed for this study. The ship track check compares the position with the six positions closest in time, and then the date is checked. If the ship speed exceeds 40 knots or the position is more than 60 nautical miles (1° latitude) away from the expected position interpolated from adjacent reports, then it is doubtful and the position or the date is corrected to a value; values of latitude and longitude (date) are changed digitally, so that the modified position (date) is close to the expected position (date). Such errors originate mainly from human error; therefore, the interpolated position (date) is not used for modification of position (date). Doubtful reports comprise 1–5% of all the reports for each year, and about half of them, mostly positions, are corrected successfully. However, the ship track check cannot be applied to about half of the reports because of missing call signs or missing ship identifications.

Biased data are discarded using a check against a blacklist to avoid anomalies being enhanced along ship tracks. The blacklist is defined in each calendar month before the objective analyses. Magnitudes of ship bias intercepted by the blacklist check exceed or are comparable to the natural standard deviations of monthly anomalies. Therefore, the procedure must be constructed carefully. In this study, only ships that definitely have erroneous data will be entered in the blacklist. If more than 80% of N data from a ship within ± 1 month are positively (negatively) biased, i.e. the values differ by more than $r\sigma$ relative to climatology, then none of that ship's data is used in the objective analyses; here, σ is the standard deviation and r is a function of the number of observations N, defined empirically as $r = 1$ for $N \geq 100, r = 2.5$ for $75 \leq N < 100$, and $r = 3$ for $30 \leq N < 75$. All data with $N < 30$ bypass this check, because it is difficult in such cases to distinguish inevitable errors from errors by chance using only the parameter r. The climatology and σ used here are described in Section 2.4. An additional parameter is introduced for SST data, because SST anomalies can persist for a long time and the daily change is small compared with those of atmospheric elements. This parameter is the longitudinal and latitudinal ranges of ship movement, or the spatial dimension of observational area by a ship, during 3 months. Considering the largest spatial scale of SST anomaly as being associated with El Niño–southern oscillation (ENSO), the longitude and latitude ranges are set to 60° and 30° respectively. A ship is entered into the blacklist if its movement exceeds both the ranges of longitudes and latitudes and if its observations of parameter r are judged to be biased. A *posteriori* blacklist statistics help detect problems in historical data. For example, SLP, wind speed, and DPT observations show more bias during World War II relative to other periods.

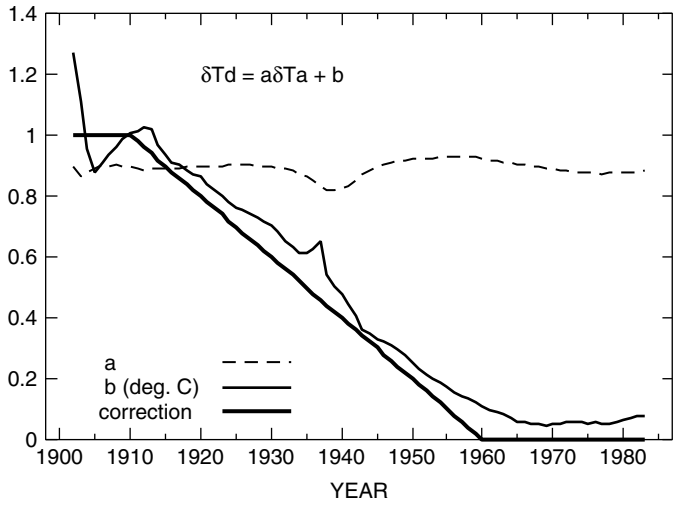

Figure 2. Positive bias of DPT observation. The thick solid curve represents global mean biases of DPT determined in this study. The other two curves are the regression coefficients a (broken) and b (thin solid) for the linear relationship between air temperature anomalies δT_a and DPT anomalies δT_d : $\delta T_d = a\delta T_a + b$

DPT observations before 1960 include a severe positive bias. The bias is larger in earlier decades, and was probably caused by dried wet bulbs or observations under airless conditions. No similar trend in DPT observations exists at stations on islands or along the coasts of Japan. Figure 2 shows the positive bias in the historical DPTs (thick solid line). A linear regression model between the deviations from climatology of DPT δT_d and AT δT_a identifies the bias. The letters a and b in the figure denote the regression coefficients of the model $\delta T_d = a\delta T_a + b$. The coefficient a is nearly constant, and b decreases with time. This result suggests that the change in b drives the positive bias, although the relationship is slightly skewed rather than linear. Therefore, in this study, the bias shown by the thick solid line is subtracted from DPT observations made before 1960.

2.4. Climatology

Climatology and the corresponding standard deviations of SST and marine meteorological variables are required for quality control and objective analyses. Here, the resolution is monthly and $1^\circ \times 1^\circ$ in the global oceans, and the climatology is carefully constructed considering data sparseness. Box averages of observations are first computed on a coarse $5^\circ \times 5^\circ$ grid in every calendar month between 1950 and 2000, and a crude monthly climatology is averaged from the above gridded data. Next, missing data in those monthly gridded fields are filled with values interpolated spatially and temporally using monthly deviations from nearby grid points. This results in a revised climatology on the coarser grid with fewer regions of missing data. The coarse climatology is then interpolated to the $1^\circ \times 1^\circ$ grid. Similarly, monthly deviations are first computed as box averages and missing deviations are then replaced by interpolated values. However, this technique does not yield a complete climatology. Therefore, two gridded databases are introduced. One includes global objective analyses for 1989–2000 of meteorological variables in the polar regions produced through data assimilation at the Japan Meteorological Agency, and the other is the NCEP OI.v2 SST for SSTs in closed seas. Thus, a climatology is finally obtained over the entire grid, and standard deviations of monthly anomalies can be computed.

2.5. The Kobe Collection

The recently digitized Kobe Collection contains 3.1 million data points for the period between 1890 and 1932. The amount of data for the Pacific Ocean between 1900 and 1932 will double in a future release of

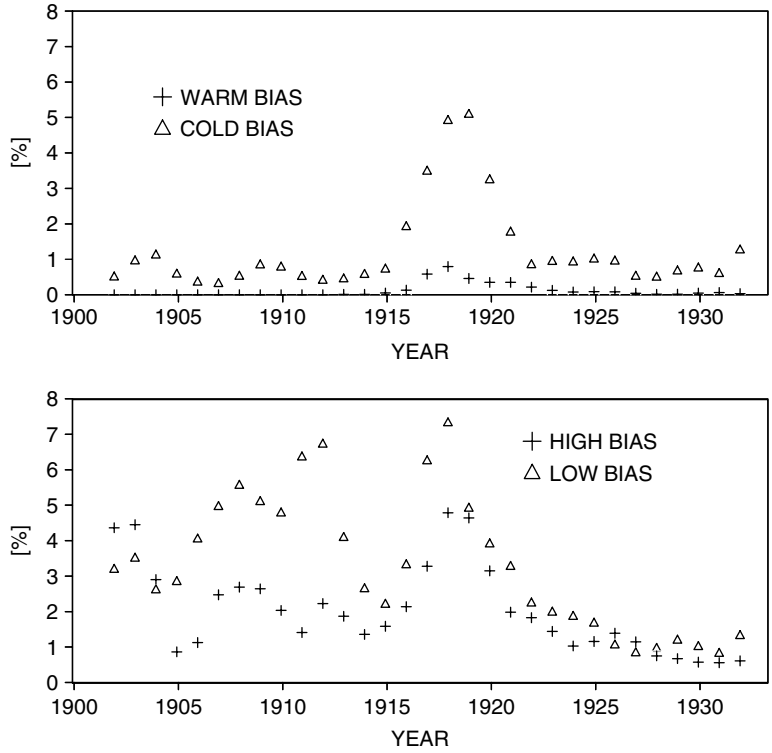

Figure 3. Yearly ratio (%) of the number of all observed data to the number of biased SST (upper) and SLP (lower) data in the Kobe Collection. Plus signs and triangles indicate positive and negative biases respectively

ICOADS that incorporates the Kobe Collection. Some metadata are included with the observed data. For instance, platform heights are used to remove wind speed trends as mentioned above. The latest version of the digitized data is distributed on CD-ROM (March 2003 edition). Objective analyses made with the Kobe Collection showed a decrease in analysis errors relative to an analysis with only ICOADS. This will be demonstrated in Section 5.

Position and date errors occur less frequently in the Kobe Collection than in ICOADS because a manual check has been applied to the data. However, the Kobe Collection includes a lot of biased data. In particular, SST data from around 1920 and SLP data from before 1921 are biased (Figure 3). The percentage of biased data is much larger than the upper limit of 1% for ICOADS. These biased data are identified in the blacklist check. The causes of the bias are unclear, although the biased data have been checked against log sheet records.

3. OBJECTIVE ANALYSIS

Objective analyses of SST and marine meteorological elements are conducted daily. The first guess, from which deviations are calculated by the objective analysis, is given by the analysis from the previous day, because the daily field more closely resembles the analysis of the previous day than the climatology (Reynolds and Smith, 1994). The analysis scheme is based on optimum interpolation (OI). Table I contains the required analysis parameters.

The parameters in Table I are estimated from observational covariances. The covariance model is represented by a rational function, $a/(1 + bx^m)$, where x is the distance or time lag between two observations, $m = 1$ for temporal coherency and $m = 2$ for spatial coherency, and a and b indicate uncertainty and coherency respectively (Ishii *et al.*, 2003). The constant a provides the ratio of the first-guess error standard deviation to that of the observational error (N/S in the table). The N/S value for SST is from Reynolds and Smith (1994),

Table I. List of analysis parameters (see text for details)

Parameter	Coherency		N/S	No. of EOFs
	Space (km)	Time (days)		
SST	600	15	4.0	89
SLP	1200	2	1.5	117
AT	800	6	2.0	63
DPT	600	3	1.9	76
U	800	2	1.1	117
$\|U\|$	700	1	1.5	90
CLOUD	600	1.5	2.0	112

because this estimate is reliable owing to the use of satellite observations and because SST is noisier than the atmospheric variables.

Standard deviations for the monthly climatology (Section 2.4) yield spatial distributions of error variances for the first guess and observation. Monthly statistics are more reliable than are daily statistics where data are sparse. The error variances of day-to-day changes are computed with two factors, given *a priori* as follows. One factor is the ratio between the error variance for the daily climatology and that of the monthly climatology computed with a temporal coherence model, assuming that the daily variance is constant in the month. The other factor, $2\{1 - C_t(1)\}$, represents the ratio of the error variance of day-to-day changes to that of the daily climatology, where $C_t(x)$ denotes the temporal coherence model. Note that the temporal scales in Table I are for the deviations for climatology, not for day-to-day changes.

Observational error variances σ_o are also given by N/S in the table and the error variance of the first guess. The error variances reduce to σ_o/N for merged data (Section 2.3), where N is the number of reports used in merging. However, the maximum N is bounded, and a reduction of observational error variance is permitted up to 50% of σ_o in order to yield a smooth analysis (Reynolds and Smith, 1994). In addition, data observed by the same ship or buoy are merged, considering there to be correlation among them (Ishii *et al*., 2003).

The analysis error of the corresponding daily analysis is also estimated within the framework of OI (e.g. Ghil and Malanotte-Rizzoli, 1991). The analysis errors for long-term averages of daily analyses are crudely computed from daily errors, assuming that the coherence models for the analysed values are the same as those for the first guesses.

The first guess $T_g(n)$ for day n is given in the objective analysis by $T_c(n) + \alpha\delta T_a(n-1)$, where $T_c(n)$ denotes climatology interpolated daily for day n, and $\delta T_a(n-1)$ is the anomaly for the previous day. Constant α is a damping factor defined for each element so that $\alpha^t = 0.5$ is satisfied. Here, t is the characteristic time scale listed in Table I.

Objective analyses for SLP and vector wind are simultaneously made with an assumption of geostrophic balance (e.g. as in Bergman (1979)). The vector wind is divided into geostrophic and nongeostrophic components, so five components are simultaneously optimized. The simultaneous analysis yields SLP and vector winds that are dynamically consistent. Furthermore, wind observations compensate for data sparseness in SLP, and vice versa. The parameter U in Table I is used to optimize the nongeostrophic wind. However, the optimization is for the full wind component and will be re-examined in a future study.

In addition to the ordinary OI analyses, a monthly reconstruction is introduced that yields gridded data with homogeneous quality and reduces observational noise in the resultant fields. Usually, reconstruction analyses are realized using *a priori* information on interannual variability with reduced degrees of freedom in space using empirical orthogonal functions (EOFs; Parker *et al*., 1995; Smith *et al*., 1996; Kaplan *et al*., 1998). Reconstruction in this study is based on a two-dimensional variational method (Ishii *et al*., 2003), in which the first-guess covariance matrix is reformulated with EOFs of monthly mean anomalies from the OI analyses. When SLP and vector winds are reconstructed, all three elements are simultaneously analysed as in the OI analysis. The rightmost column in Table I shows the number of EOFs used in the reconstruction; the

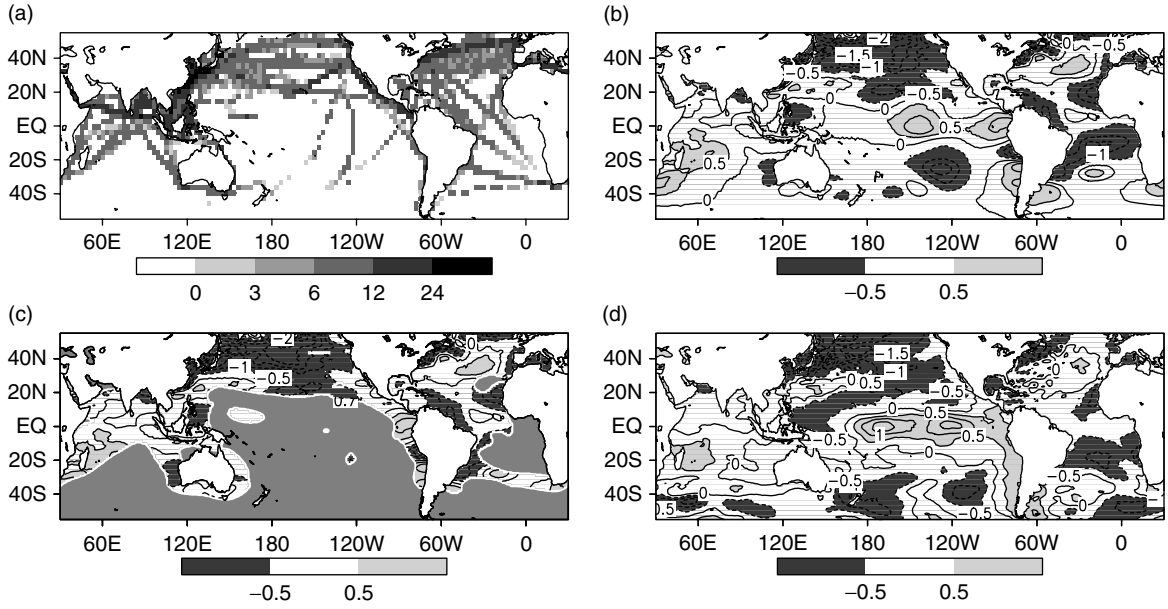

Figure 4. Sample objective analysis results. (a) The number of data used in the averaged daily analysis for January 1919. (b) Monthly mean temperature anomalies (°C) relative to climatology as revealed by the OI. Contours are shown every 0.5 °C; areas with anomalies greater than 0.5 °C and less than −0.5 °C are shaded lightly and darkly respectively. (c) As (b), but masked with analysis errors for the monthly mean anomalies. Areas of missing data occur where the analysis error variance exceeds 50% of the first-guess error variance. (d) As (b), but for the reconstructed SST

EOFs represent 80% of the variance in the OI analyses between 1961 and 2000. Trends in the OI analyses are subtracted during the computation of EOF and are treated separately in the reconstruction.

Historical analyses were prepared using OI and reconstruction for all variables in Table I over the global oceans. Monthly averages of the daily analyses are presented next.

The analysis database in this study contains analysed values, analysis errors, and the distribution of data used in the objective analysis. Figure 4 shows the monthly mean SST for January 1919. The analysed SST anomalies shown in Figure 4(b) include sizable and widely spread deviations from climatology along major ship routes (Figure 4(a)). The analysis errors computed by OI can be used as a measure of the reliability of the analysis products, as shown in Figure 4(c). Figure 4(a) and (c) show the same SST analysis, but the values in Figure 4(c) are masked by the analysis error, the variance of which is greater than 50% that of the first guess. The distribution of daily observations during the month is considered when the analysis error is computed. It is found in the figure that the monthly mean analysis by OI is not always reliable along routes of ships. Figure 4(d) contains the reconstruction analysis. The SST anomalies in Figure 4(d) are similar to those in Figure (b), but wedge-shaped anomalies related to an El Niño event are clearly analysed over the tropical Pacific in Figure 4(d).

4. TREND

4.1. Marine temperatures and cloud cover

Figure 5 shows time series of global mean SST, NAT, DPT, and total cloud cover from the OI analyses. Monthly values are plotted and are smoothed with 25 month running averaging. The figure contains notable features: increasing trends, local peaks in the early 1940s, and interannual variations in marine temperatures. Linear trends are approximately $0.53 \pm 0.05\,^{\circ}\mathrm{C}/100$ years, $0.47 \pm 0.05\,^{\circ}\mathrm{C}/100$ years, and $5.0 \pm 0.3\%/100$ years respectively for SST, NAT, and total cloud cover. DPT trends are not given

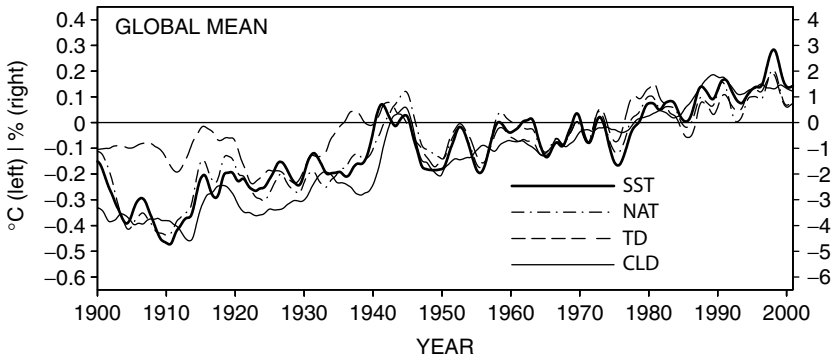

Figure 5. Time series of global mean SST (thick solid; °C), NAT (dash-dotted; °C), DPT (dash; °C), and total cloud cover (thin solid; %) anomalies relative to 1961–90 averages. The time series are smoothed by 25 month running averaging

owing to a lack of DPT data before 1920 and in the late 1930s (Figure 1). The SST trend is comparable to that of HadISST, which we estimate to be 0.50 °C/100 years. During the last two decades, NAT appears to be cool relative to the SST (Rayner *et al*., 2003), so that the NAT trend is slightly smaller than that of the SST.

Norris (1999) discussed causes of global ocean cloud cover for the years from 1952 to 1995, carefully considering artificial effects on the positive trend for *daytime* data. He concluded that trends in low clouds may be responsible for increases in total cloud cover. The present study also reveals that the frequency of low clouds covering 5–8 oktas in the *night-time* increases during the later decades as much as in the daytime. Accordingly, cloud cover trends in the present analysis are statistically enhanced by the use of data from both day and night. Note also that reports of sky obscured mainly by fog, coded as 9 in ICOADS, have increased since the 1940s and that obscuration at night is in 10% of all data in the 1980s. Such obscured data are converted in this study to 100% cloud cover. In addition, cloud cover observations at night are affected by moonlight (Hahn *et al*., 1995). Therefore, it is better in a future study that the night-time data for an obscured sky are discarded, and all night-time data will be referenced to moonlit periods. There is a local minimum in cloud cover during the latter half of the 1930s. Cloud observations with source identification of 93 in ICOADS are withheld in the present analysis. Otherwise, the global mean cloud cover decreases by 2% more in the years 1935–39 according to our analysis. A change in the cloud reporting unit from tenths to oktas (Elms *et al*., 1994) may have affected the observations of low cloud, but the problems with the cloud cover observations are not fully understood at present.

An El Niño event occurred from the late 1930s to the early 1940s, as is suggested by wedge-shaped, positive SST anomalies in the eastern tropical Pacific; horseshoe-shaped positive anomalies in the tropical Pacific accompanied the subsequent La Niña event. ENSO indices are constructed with the present analyses and discussed in Section 6.2. The local peaks of the global mean SST are affected by those events and by the ICOADS biases discussed in Section 2.3. During World War II, observations were sparse (Figure 1), and the spatial distribution of the data changed drastically. In particular, few observations occurred in the North Pacific and North Atlantic. Therefore, ENSO-induced anomalies may be overestimated in the global mean. In contrast, the peaks in NAT and total cloud cover occurred in the mid-1940s. The NAT peak is associated with NAT observation errors discussed by Folland *et al*. (1984), even though all NAT observations have been corrected (Section 2.3). A correction of greater than 0.5 °C should be subtracted from the NAT observations, especially in the tropical and North Pacific and in the North Atlantic. However, this is just an adjustment, and the NAT observations themselves are doubtful during the period.

4.2. SLP and surface wind

There are artificial trends of SLP and surface wind in the present analyses. As shown in Figure 6(b), analysed SLPs have significant positive trends at high latitudes in both hemispheres. Negative SLP anomalies

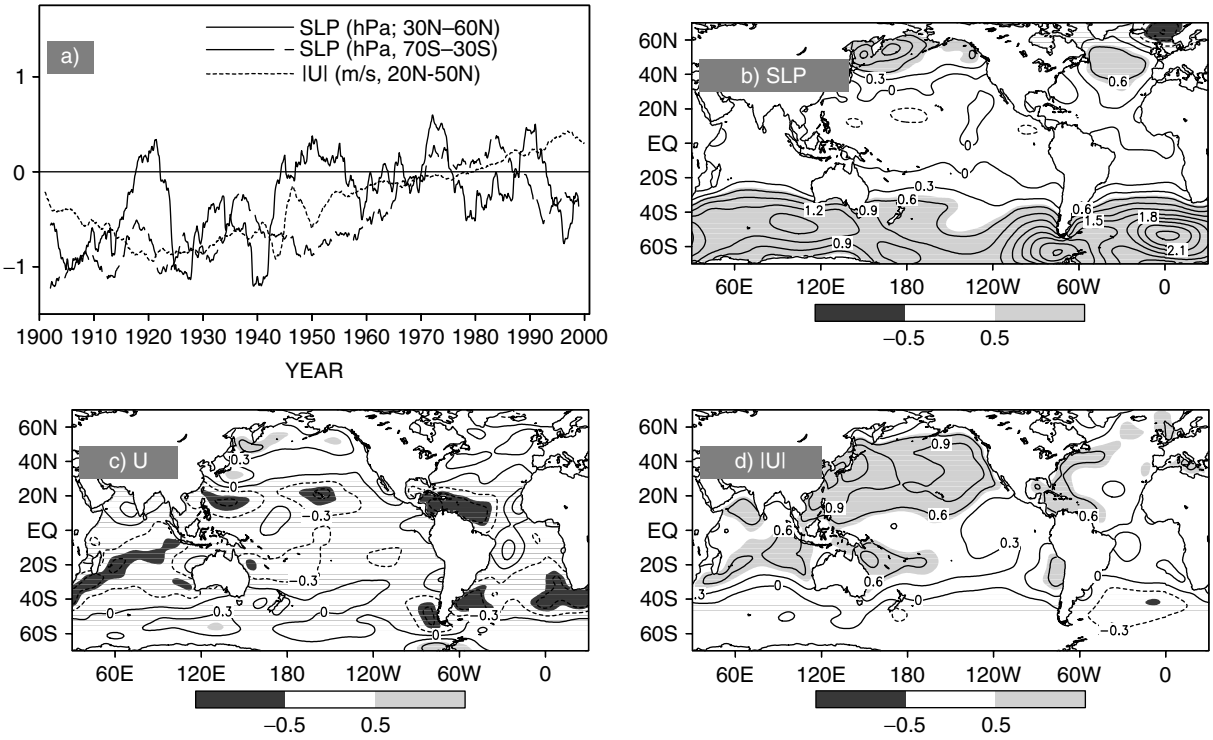

Figure 6. (a) Time series of zonal averages of SLP from 30°N to 60 °N (solid; *hPa*), SLP from 70 °S to 30 °S (broken), and wind speed from 20 °N to 50 °N (dotted; m/s). Linear trends in (b) SLP (hPa), (c) zonal wind speed (m/s), and (d) scalar wind (m/s)

appear before 1945 for zonal means between 30 and 60°N and before 1960 between 70 and 30 °S, as shown by the solid and broken lines respectively in figure 6(a). SLP cannot have a global trend unless the atmosphere is gaining or losing mass. Trends are primarily caused by data biases. Negative biases in SLP observations in the Kobe Collection (Figure 3) cause some of the positive trends over the western North Pacific, because all biased observations are not rejected by the blacklist check. The trend in SLP observations, averaged zonally between 70 °S and 30 °S, is large for strong winds during the period. One reason for the low pressure biases might be 'suction', as suggested by Hayashi (1974), created when air flows from inside a ship leeward to the outside, although further investigation is necessary to show this. The time series over the North Pacific (thick line in Figure 6(a)) includes an interdecadal variation related to the Pacific decadal oscillation (Mantua *et al*., 1998; Minobe and Maeda, 2005).

Zonal winds have a weak negative trend, especially apparent at low latitudes (Figure 6(c)), i.e. increasing trade winds (Whysall *et al*., 1987). Scalar winds also show statistically significant trends, especially in the North Pacific (Figure 6(d) and dotted line in Figure 6(a)). Biases linked to historical changes in anemometer heights have been subtracted and the modified Beaufort scale is adopted in the analysis. However, there were fewer opportunities for reporting winds exceeding 5 m/s during the first half of the century than during the second half of the century. Furthermore, there was no standardized Beaufort scale before World War II (Ramage, 1987; Cardone *et al*., 1990), which may be a major reason for low wind speeds before 1950. The use of the modified Beaufort scale (Lindau, 1994) yields an increase of about +0.2 m/s in the hemispheric average of the scalar wind before 1950. Winds also increase during the last three decades owing to the possible underestimation of the anemometer height trend (Section 2.3). It is also possible that during this period the mixing of anemometer readings and estimated winds may be problematic for observations with a wind speed indicator of 3 in ICOADS (wind reported in knots and estimated) for 1970–2000, and indicator 6 (units unknown and unknown method) for 1940–60. The

average observational anomaly increases by about 0.5–1.5 m/s for the periods in question in many of ocean basins.

5. IMPACT OF THE KOBE COLLECTION

Another analysis error is introduced in this section to highlight the impact of the Kobe Collection on the objective analyses. The analysis error calculated during the objective analyses is not used here because the observational error is underestimated owing to the use of the merging procedure (Section 3). This will, therefore, underestimate the impacts of the Kobe Collection. The following equation is derived following OI theory, but the number of observations is not reduced for all observations available for the objective analysis.

Figure 7 shows the expected reduction of the analysis error standard deviation averaged for 1903–32 by using both the Kobe Collection (K) and ICOADS (I). The reduction is $1 - \sigma_a(I + K)/\sigma_a(I)$, where $\sigma_a(I + K)$ and $\sigma_a(I)$ are analysis error standard deviations with and without the Kobe Collection respectively. Assuming first-guess errors are independent of both each other and of observational errors, the equation $(\sigma_a^2)^{-1} = (\sigma_g^2)^{-1} + (\sigma_o^2/N)^{-1}$ is obtained, where σ_g^2 and σ_o^2 are error variances for the first guess and observation respectively, and N is the number of all observations. Let σ_g^2 be the variance for interannual variability here rather than for day-to-day changes. Additionally, $\sigma_o = \sigma_g$ is assumed. The reduction is computed on a monthly $2^\circ \times 2^\circ$ grid. The figure shows reductions of more than 10% in SST (upper) and SLP (lower) in the seas around Japan, in the South China Sea, and along major ship routes in the global oceans. The merit of using this reduction is to convert the number of data points to a relevant physical quantity and to interpret values related to the objective analysis.

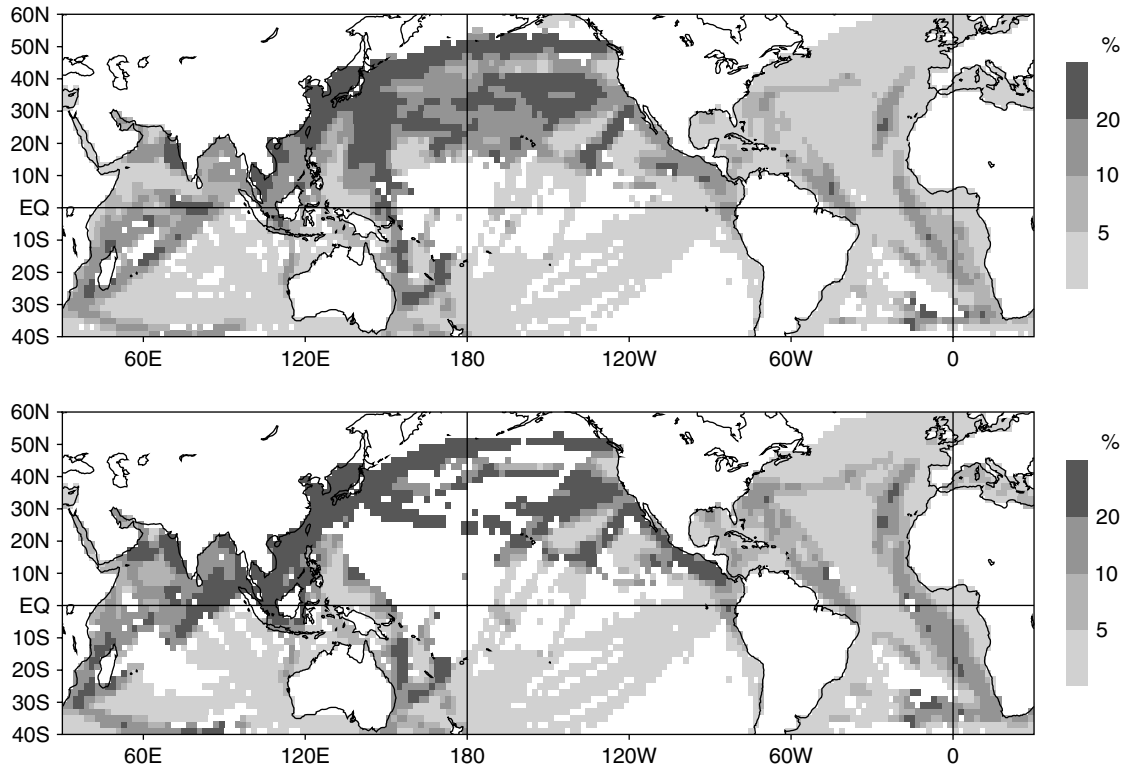

Figure 7. Reduction (%) of analysis error of SST (top) and SLP (bottom) averaged for 1903–82. Blank areas are data voids in the Kobe Collection

6. INTERCOMPARISON

6.1. SST analysis

Figure 8 compares the OI SST analysis and the NCEP OI.v2 SST using common statistics. Mean differences between the two SST analyses rarely exceed 0.2 °C (Figure 8(a)). Root-mean-square differences (RMSDs) are proportional to the standard deviation of the interannual variability: differences are small in the western tropical Pacific and large near the Kuroshio and Gulf Stream ((b)). Correlation coefficients between the two exceed 0.9 over many global oceans and also around marginal sea-ice areas because of the use of SIC

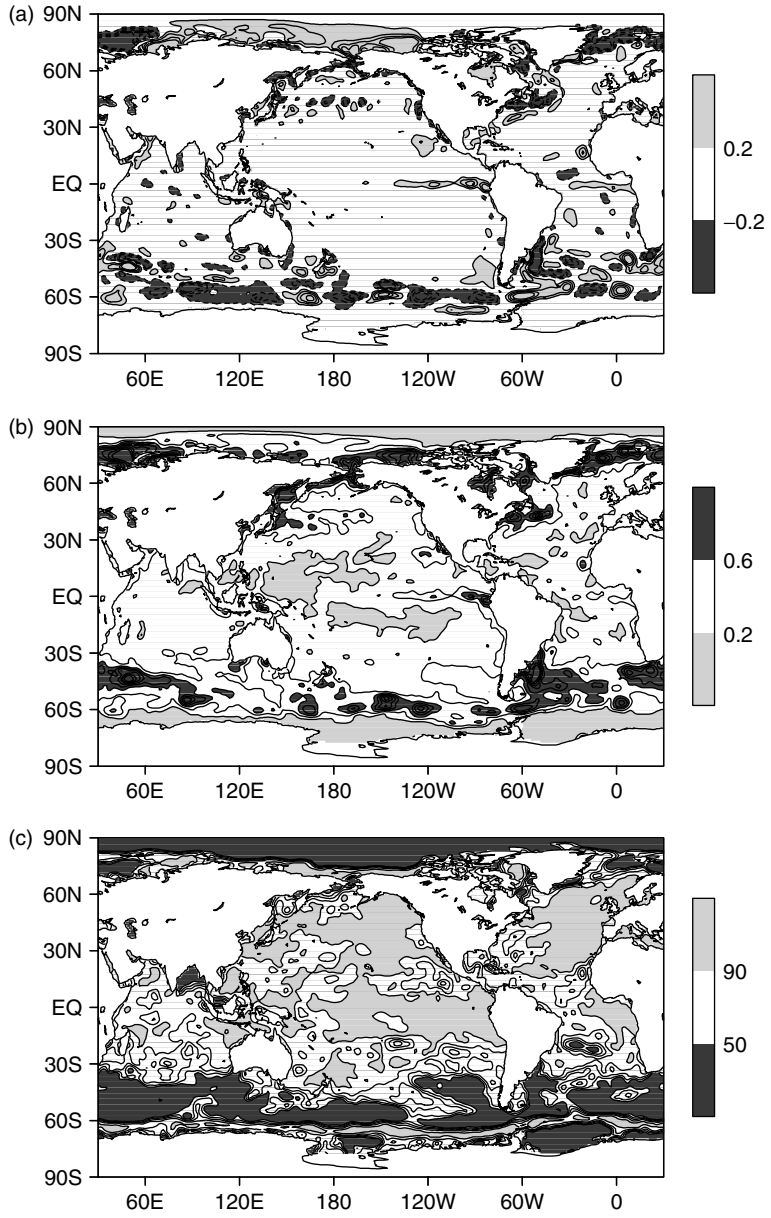

Figure 8. OI SST analysis compared with NCEP OI.v2 for years from 1982 to 2001: (a) mean difference for July (COBE minus NCEP OI.v2; °C), (b) RMS difference (°C), and (c) anomaly correlation coefficient (%). Contour interval is 0.2 °C in (a) and (b), and 10% in (c). Zero contours are not shown in (a). Legends on the right-hand side describe the shadings and threshold values

(Figure 8(c)). Correlations of less than 50% occur in the Bay of Bengal, where observations are sparse, especially in the 1990s. As no satellite data are used in the OI SST analysis, there is less variability than in the NCEP OI.v2, and large disagreements occur south of 30 °S.

6.2. ENSO indices

Several ENSO indices are computed from the reconstruction analyses. Figure 9(a) shows Niño-3 (150–90 °W, 5 °S–5 °N) SST anomalies of COBE plotted together with those of HadISST. El Niño and La Niña events alternate with a 3–6 year cycle throughout the century, and the two curves agree very well. The analysis error, which is not shown in the figure, is about 0.2 °C after the 1960s. Before 1960, errors are larger than 0.3 °C, exceeding 0.5 °C during the two world wars.

There are no analysed values on land in COBE. A southern oscillation index (SOI) from COBE is constructed using SLP analysis data at the two grid points nearest Darwin and Tahiti, to allow comparisons with the SOI maintained by the Bureau of Meteorology of Australia. The two SOI curves show good agreement (Figure 9(b)).

In the central Pacific, strong westerlies appear around deep convection during El Niño events; easterlies dominate during La Niña events. Zonal wind averaged in the Niño-4 region (160 °E–150 °W, 5 °S–5 °N) in the COBE analysis is in phase with Niño-3 SST anomalies in HadISST.

The results from the OI analysis show similarities to Figure 9(a) and (b). However, the variance of the zonal wind in the OI analysis is much smaller than in the reconstructed analysis (Figure 9(c)) because wind data are sparse. Furthermore, the geostrophic assumption used in the OI analysis fails at low latitudes. An SST index averaged in the western Pacific (0–14 °N, 130–150 °E) is affected by observational noise in the OI analysis. That noise is efficiently smoothed by the reconstruction.

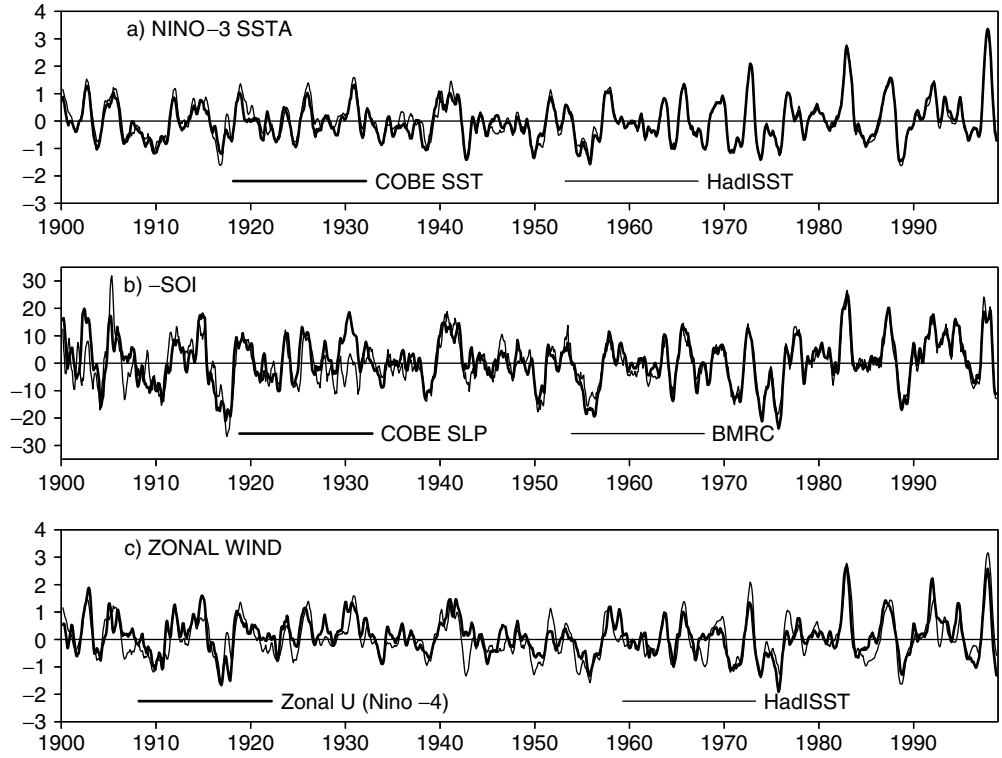

Figure 9. Time series of ENSO indices. (a) Niño-3 SST anomaly (°C), (b) negative SOI, and (c) zonal wind averaged over Niño-4 region (m/s). The indices of COBE (thick) are compared with those of HadISST and the Bureau of Meteorology of Australia (thin). Anomalies are defined as departures from 1961–90 averages

7. CONCLUDING REMARKS

Objective analyses of SST and marine meteorological variables have been carried out using 102 years of data. The objective analyses yield a gridded dataset that can be used to validate the quality of historical observations.

Global warming trends are present in the global mean SST, NAT, DPT, and total cloud cover. Spurious trends appear in SLP and scalar winds. ENSO indices are widely used to highlight atmospheric and oceanic conditions in the equatorial Pacific. The reconstruction scheme developed in this study reduces the observational noise, yields good estimates of the ENSO indices, and successfully reproduces typical climate anomalies over the tropical Pacific.

Maritime observations are not common enough to allow a comprehensive description of spatial and temporal variations at the sea surface. Furthermore, metadata are also scarce. The Kobe Collection, digitized by the Japanese community, contributes data from 1900 to 1932 in data-sparse regions of ICOADS. The Kobe Collection data fill gaps, particularly those around World War I. The collection also includes metadata, such as platform heights, which are useful for inferring ship sizes.

Some problems with objective analyses using historical observations remain unsolved. Such problems can be caused by either the observations themselves or observational uncertainties. Uncertainties can have a dramatic impact on analysis when data are sparse. The uncertainty can be evaluated objectively by estimating analysis errors, for instance. Further investigation is warranted to heighten understanding of the historical background of marine observations and to homogenize the quality of historical observations. Only the monthly mean analyses are verified in this study. It is necessary to study reliability of daily analyses with sparse data, particularly with data before 1950. The accuracy of analysed data by OI and reconstruction will be quantified by using cross-validation (e.g. Smith *et al*., 1996) in a future study.

Several applications using the COBE products have begun. The SST analyses are being used in the Japan Reanalysis project, which seeks to produce a high-quality climatological dataset to enhance seasonal prediction modelling and climatological studies. Air–sea fluxes can be computed from the elements analysed. Thus, the COBE products are now used as forcing to ocean general circulation models to reveal flux forcing effects. The analysis database includes analysis errors and the number of data used in the analyses. This information will be helpful to users of the products. All of the output is available for climate study.

ACKNOWLEDGEMENTS

We wish to thank the sources of data used in this study: ICOADS (Mr S. J. Worley, CDC/NOAA, USA), buoy observations (Dr B. Bradshaw, MEDS, Canada), HadISST and correction data for historical SSTs (Met Office, UK), sea-ice data (Dr J. E. Walsh and Dr. B. Chapman, University of Illinois, USA), SST OI.v2 analysis (NCEP/NOAA, USA), and SOI data (Bureau of Meteorology, Australia). The manuscript has been prepared with encouragement and help from Ms T. Manabe (WMO) and Mr S. Woodruff (CDC/NOAA, USA). We greatly appreciate the generous support from Professor M. Kimoto (CCSR, University of Tokyo) and staff members of CCSR, and thank an anonymous reviewer for thoughtful and encouraging comments on the manuscript.

REFERENCES

Bergman KH. 1979. Multivariate analysis of temperature and wind using optimum interpolation. *Monthly Weather Review* **107**: 1423–1444.

Cardone VJ, Greenwood JG, Cane MA. 1990. On trends in historical marine wind data. *Journal of Climate* **3**: 113–127.

Cavalieri DJ, Gloersen P, Campbell WJ. 1984. Determination of sea ice parameters from NUMBUS-7 SMMR. *Journal of Geophysical Research* **89**: 5355–5369.

Cavalieri DJ, Corawford JP, Drinkwater MR, Eppler DT, Farmer LD, Jentz RR, Wackerman CC. 1991. Aircraft active and passive microwave validations of sea ice concentrations from the DMSP SSM/I. *Journal of Geophysical Research* **96**: 21 989–22 008–.

Cavalieri DJ, Parkinson CL, Gloersen P, Comiso JC, Zwally HJ. 1999. Deriving long-term time series of sea ice cover from satellite passive-microwave multisensor data sets. *Journal of Geophysical Research* **104**: 15 803–15 814–.

Da Silva AM, Young CC, Levitus S. 1994. Toward a revised Beaufort equivalent scale. In *Proceedings from the COADS Winds Workshop*, Kiel, Germany.

Elms JD, Woodruff SD, Worley SJ, Hanson C. 1994. Digitizing historical records for the Comprehensive Ocean–Atmosphere Data Set (COADS). *Earth System Monitoring* **4**: 4–10.
Esbensen SK, Kushnir Y. 1981. The heat budget of the global ocean: an atlas based on estimates from surface marine observations. Oregon State University, Corvallis, OR.
Folland C. 2003. Assessing bias corrections in historical sea surface temperature using a climate model. In *Proceedings of Second JCOMM Workshop on Advances in Marine Meteorology*, Brussels, Belgium, 17–22 November. WMO/TD-No. 1199; 13.
Folland CK, Parker DE. 1995. Correction of instrumental biases in historical sea surface temperature data. *Quarterly Journal of the Royal Meteorological Society* **121**: 319–367.
Folland CK, Parker DE, Kates FE. 1984. Worldwide marine temperature fluctuations 1856–1981. *Nature* **310**: 670–673.
Ghil M, Malanotte-Rizzoli P. 1991. *Data Assimilation in Meteorology and Oceanography*. *Advances in Geophysics*, Vol. 33. Academic Press: 141–266.
Hahn JJ, Warren SG, London J. 1995. The effect of moonlight on observation of cloud cover at night, and application to cloud climatology. *Journal of Climate* **8**: 1429–1446.
Hanawa K, Yasunaka S, Manabe T, Iwasaka N. 2000. Examination of correction to historical SST data using long-term coastal SST data taken around Japan. *Journal of the Meteorological Society of Japan* **78**: 187–195.
Hayashi S. 1974. Some problems in marine meteorological observations, particularly of pressure and air temperature. *Japan Meteorological Agency, Journal Meteorological Research, Japan Meteorological Agency* **26**: 84–87 (in Japanese).
Hellerman S, Rosenstein M. 1983. Normal monthly wind stress over the world ocean with error estimates. *Journal of Physical Oceanography* **13**: 1093–1104.
Ishii M, Kimoto M, Kachi M. 2003. Historical ocean subsurface temperature analysis with error estimates. *Monthly Weather Review* **131**: 51–73.
Kaplan A, Cane MA, Kushnir Y, Clement AC. 1998. Analyses of global sea surface temperature 1856–1991. *Journal of Geophysical Research* **103**: 18 567–18 589–.
Komura K, Uwai T. 1992. The collection of historical ships' data in Kobe Marine Observatory. *Bulletin of Kobe Marine Observatory* **211**: 19–30.
Kutsuwada K. 1998. Impact of wind/wind-stress field in the North Pacific constructed by ADEOS/NSCAT data. *Journal of Oceanography* **54**: 443–456.
Lindau R. 1994. Rapport on Beaufort equivalent scales. In *Proceedings from the COADS Winds Workshop*, Kiel, Germany.
Manabe T. 1999. The digitized Kobe Collection, phase I: historical surface marine meteorological observations in the archive of the Japan Meteorological Agency. *Bulletin of the American Meteorological Society* **80**: 2703–2715.
Mantua NJ, Hare SR, Zhang Y, Wallace JM, Francis RC. 1998. A Pacific interdecadal climate oscillation with impacts on salmon production. *Bull. Amer. Meteor. Soc.* **25**: 1297–1300.
Minobe S, Maeda A. 2005. A 1° monthly gridded sea-surface dataset compiled from ICOADS from 1850 to 2002 and Northern Hemisphere frontal variability. *International Journal of Climatology* **25**: 881–894; this issue.
Norris JR. 1999. On trends and possible artifacts in global ocean cloud cover between 1952 and 1995. *Journal of Climate* **12**: 1864–1870.
Parker DE, Folland CK, Bevan A, Ward MN, Jackson M, Maskell K. 1995. Marine surface data for analysis of climate fluctuations on interannual to century time scales. In *Natural Climate Variability on Decade to Century Timescales*. National Academy Press: 241–250.
Ramage CS. 1987. Secular change in reported surface wind speeds over the ocean. *Journal of Climate and Applied Meteorology* **26**: 525–528.
Rayner NA, Parker DE, Horton EB, Folland CK, Alexander LV, Rowell DP, Kent EC, Kaplan A. 2003. Global analyses of sea surface temperature, sea ice, and night marine air temperature since the late nineteenth century. *Journal of Geophysical Research* **108**(D14): 4407. DOI: 10.1029/202JD002670.
Reynolds RW, Smith TM. 1994. Improved global sea surface temperature analyses using optimum interpolation. *Journal of Climate* **7**: 929–948.
Reynolds RW, Rayner NA, Smith TM, Stokes DC, Wang W. 2002. An improved *in-situ* and satellite SST analysis for climate. *Journal of Climate* **15**: 1609–1625.
Smith TM, Reynolds RW, Livezey RE, Stokes DC. 1996. Reconstruction of historical sea surface temperatures using empirical orthogonal functions. *Journal of Climate* **9**: 1403–1420.
Walsh JE, Chapman WL. 2001. 20th-century sea-ice variations from observational data. *Annals of Glaciology* **33**: 444–448.
White WB. 1995. Design of a global observing system for gyre-scale upper ocean temperature variability. *Progress in Oceanography* **36**: 169–217.
Whysall KDB, Cooper NS, Bigg GR. 1987. Long-term changes in the tropical Pacific surface wind field. *Nature* **327**: 216–219.
Woodruff SD, Diaz HF, Elms JD, Worley SJ. 1998. COADS release 2 data and metadata enhancements for improvements of marine surface flux fields. *Physics and Chemistry of the Earth* **23**: 517–526.
World Meteorological Organization. 1970. The Beaufort scale of wind force. Reports on Marine Science Affairs, Report No. 3, WMO, Geneva.
World Meteorological Organization. 1973–1999. International list of selected, supplementary and auxiliary ships. WMO Publication 47. WMO, Geneva.
World Meteorological Organization. 1990. *Manual on Marine Meteorological Services. Volume 1, Global Aspects*. WMO No. 558. WMO: Geneva.
Yamamoto R, Sakai T. 2000. An advantage of marine meteorological data in climate change detection. In *Proceedings of International Workshop on Preparation, Processing and Use of Historical Marine Meteorological Data*; 3–8.

